

Adrian Hierro, Miguel Montes Bajo, Julen Tamayo-Arriola, Maxime Hugues, J. M. Ulloa, N. Le Biavan, Romain Peretti, François Julien, Jerome Faist, Jean- Michel Chauveau, "Intersubband transitions and many body effects in ZnMgO/ZnO quantum wells," Proc. SPIE 10533, Oxide-based Materials and Devices IX, 105331K (23 February 2018)

Copyright 2018 Society of Photo-Optical Instrumentation Engineers. One print or electronic copy may be made for personal use only. Systematic reproduction and distribution, duplication of any material in this paper for a fee or for commercial purposes, or modification of the content of the paper are prohibited.

<http://dx.doi.org/10.1117/12.2290640>

PROCEEDINGS OF SPIE

[SPIDigitalLibrary.org/conference-proceedings-of-spie](https://spiedigitallibrary.org/conference-proceedings-of-spie)

Intersubband transitions and many body effects in ZnMgO/ZnO quantum wells

Hierro, Adrian, Montes Bajo, Miguel, Tamayo-Arriola, Julen, Hugues, Maxime, Ulloa, J. M., et al.

Adrian Hierro, Miguel Montes Bajo, Julen Tamayo-Arriola, Maxime Hugues, J. M. Ulloa, N. Le Biavan, Romain Peretti, François Julien, Jerome Faist, Jean-Michel Chauveau, "Intersubband transitions and many body effects in ZnMgO/ZnO quantum wells," Proc. SPIE 10533, Oxide-based Materials and Devices IX, 105331K (23 February 2018); doi: 10.1117/12.2290640

SPIE.

Event: SPIE OPTO, 2018, San Francisco, California, United States

Intersubband transitions and many body effects in ZnMgO/ZnO quantum wells

Adrian Hierro^a, Miguel Montes Bajo^a, Julen Tamayo-Arriola^a, Maxime Hugues^b, J.M. Ulloa^a, N. Le Biavan^b, Romain Peretti^c, François Julien^d, Jérôme Faist^c, Jean-Michel Chauveau^b

^aISOM-Universidad Politecnica de Madrid, Avenida Complutense 30, Ciudad Universitaria, 28040 Madrid, Spain; ^bUniversite Cote d'Azur, CNRS, CRHEA, 06560 Valbonne, France; ^cInstitute for Quantum Electronics, ETH Zurich, Wolfgang-Pauli-Strasse 16, 8093 Zurich, Switzerland; ^dC2N at the University Paris-Sud, University Paris-Saclay, rue Ampère, Orsay, France.

ABSTRACT

In this work we show the potential of the ZnO/ZnMgO material system for intersubband (ISB)-based devices. This family of alloys presents a unique set of properties that makes it highly attractive for THz emission as well as strong coupling regimes: it has a very large longitudinal optical phonon energy of 72 meV, it can be doped up to $\sim 10^{21}$ cm⁻³, it is very ionic with a large difference between the static and high frequency dielectric constants, and it can be grown homoepitaxially on native substrates with low defect densities. The films analyzed here are grown by molecular beam epitaxy (MBE) on a non-polar orientation, the m-plane, with varying QW thicknesses and 30% Mg concentrations in the barrier, and are examined with polarization-dependent IR absorption spectroscopy. The QW band structure and the intersubband transitions energies are modeled considering many body effects, which are key to predict correctly the measured values.

Keywords: ZnO, ZnMgO, intersubband, terahertz, infrared, homoepitaxy, non-polar

1. INTRODUCTION

ZnO-based QWs have recently started to show their potential for intersubband devices working from the mid-IR to the THz spectral regions^{1,2,3,4}. Particularly, through the ZOTERAC project (www.zoterac.eu), funded by the European Commission, we have started to give the first steps towards THz emission with quantum cascade lasers (QCLs), and detection with quantum well infrared detectors (QWIPs) and quantum cascade detectors (QCDs). All these devices use the concept of an optical transition within energy levels of the same band, typically the conduction band, and thus only require of one type charge carrier: electrons⁵. These type of devices are therefore unipolar, avoiding the issues and limitations that arise with p-type doping in ZnO and related oxides. Here we show that ZnO/ZnMgO QWs can readily be grown by MBE with a very high control over the QW thickness, doping, and interface, as well as Mg incorporation in the barrier¹. Moreover, reaching the THz spectral region with ZnO should benefit from its very high longitudinal optical (LO) phonon, 72 meV (or 590 cm⁻¹)⁶, around twice that of GaAs, the dominant technology in this type of intersubband devices. Not only the LO phonon energy is quite large, but the very high ionicity of this semiconductor yields very low values of the background dielectric constant (ϵ_∞), which together with the high achievable dopings, should yield a very high coupling coefficient between phonons and the intersubband transitions². This coupled system is the so called intersubband polaron.

One of the problems that arise with ZnO is that unlike GaAs, its wurtzite structure presents an internal electric field parallel to the c-axis, which has a direct impact decreasing the oscillator strength of the QW transitions, and also affecting the QW energy, through the quantum confined Stark effect. This issue can be overcome in this type of wurtzite crystal structure if one uses a non-polar orientation of the crystal, where the c-axis and the internal electric field is parallel and not perpendicular to the QWs⁷. This is done in our case using m-plane MQWs homoepitaxially grown on m-ZnO substrates.

2. DESCRIPTION OF THE SAMPLES

The samples analyzed here were grown by molecular beam epitaxy on m-plane ZnO substrates, and consist of a ZnMgO (30% Mg) buffer layer on top of which 15-20 ZnO/ZnMgO QWs were grown, also with 30% Mg in the barriers. The barrier thickness is 10-15 nm and the QW thicknesses were varied from 2.7 to 3.7 nm. In order to enhance intersubband absorption, the doping of the QW is controlled to achieve an electron concentration of $\sim 1 \times 10^{19} \text{ cm}^{-3}$, such that the Fermi energy is found between the first and second QW energy levels, and thus only the first level is populated, whereas the rest of levels are left unpopulated. In order to couple the light into the QWs meeting the intersubband absorption selection rule, by which the electric field has to be polarized perpendicular to the QWs, multipass waveguide samples were prepared. These waveguides had two facets mechanically polished to optical quality, both at 45° to allow coupling of p-polarized light, and the substrate was also polished to optical quality to allow the internal reflection. The waveguides were processed such that the propagation of light happened perpendicular to the c-axis.

3. DESIGN OF THE SAMPLES

The control of two key parameters is needed in order to obtain intersubband absorption: the QW thickness and the barrier height. Moreover, one has to account for the fact that the ZnO reststrahlen band is found between 409 and 590 cm^{-1} , and in this spectral region the material is so opaque there is no light detection at the other end of the waveguide. Multiphonon absorption also strongly appears at higher energies than the reststrahlen band, and thus can also shadow the observation of the intersubband transitions. Thus, and as a first step, we seek for transitions in the mid-IR, below $10 \mu\text{m}$ in wavelength. Since different combinations of QW thickness and Mg contents in the barrier can lead to intersubband absorption in the mid-IR, we model first the different transitions. To do so, one has to account for the effective mass of ZnO, 0.24^6 , and for that of the barrier, which is Mg dependent, which we take to be $0.28^{3,4}$.

Regarding the effect of the barrier, the bandgap of ZnMgO needs be known together with the band offset between ZnO and ZnMgO. One of the major issues with ZnO and also ZnMgO is that the excitonic bandgap is different from the real bandgap, and also that the exciton binding energy changes with Mg content in the ternary. There are different reports on the subject, but the work by Neumann et al.⁸ clearly shows experimentally that the ZnMgO bandgap increases roughly by $25 \text{ meV}/\% \text{Mg}$. This value is actually not far from that reported from modeling by Yin et al.⁹, where they obtain $23 \text{ meV}/\% \text{Mg}$. Here we use the former value for all calculations.

To model correctly the intersubband transitions in these alloys, the additional issue is that the ZnO/ZnMgO conduction band offset is not well known. There are only a few reports on the topic from which, somehow indirectly, conduction band offset values in the $0.65\text{-}0.70 \cdot \Delta E_g$ are obtained^{3,4,9}. As we will show below, using a value of 0.67 , halfway between the reported numbers, yields good agreement with the experimentally observed transitions.

Figure 1 shows the effect that the variation of the QW thickness and Mg content in the barrier have on the intersubband transition between the first two confined levels. As shown in the figure, in order to achieve emission in the mid-IR a QW thickness in the $3\text{-}4 \mu\text{m}$ range can be used provided that the Mg content in the barrier is increased up to 30% . Thus, the samples were designed with QW thickness varying from 2.7 to 3.7 nm , keeping the Mg content in the barrier constant at 30% .

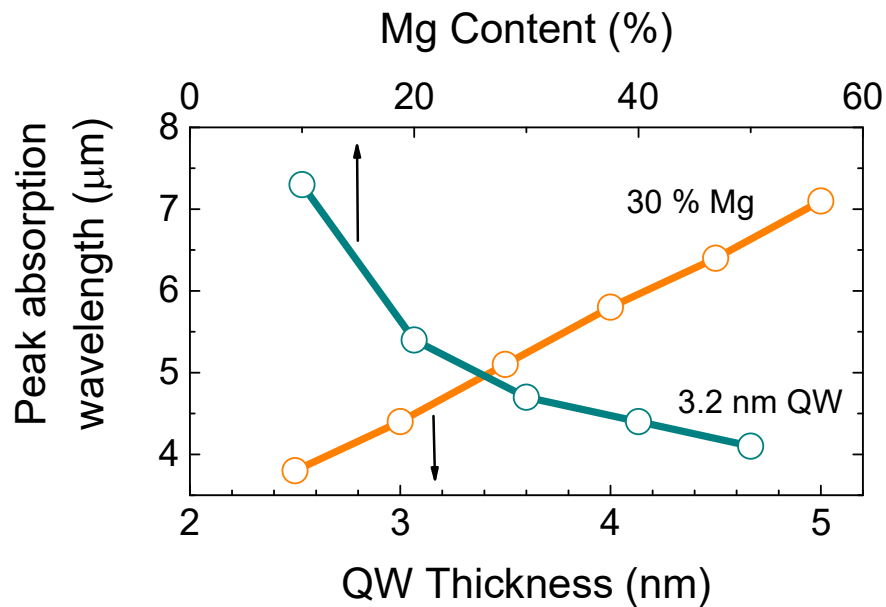


Figure 1. Calculated dependence of the intersubband absorption wavelength on the QW thickness and Mg content in the barrier.

4. ISBT RESULTS

The absorption of the MQW structures processed as multipass waveguides was measured with both s- and p-polarized light in a Fourier Transform Infrared spectrometer. Taking the p-to-s polarized spectra ratio allows to get rid of the effect of the substrate absorption as well as from free carrier absorption in the QWs, and thus the intersubband absorption can clearly be observed. Figure 2 shows the results from three QWs where only the QW thickness has been changed from 2.7 to 3.7 nm¹. The intersubband transitions have well defined absorption peak wavelengths from 3 to 5 μm, and show a full width at half maximum around 750-800 cm⁻¹. The peak energy clearly shifts to lower energy for increasing QW thicknesses, indicating that a very high control over the QW thickness is viable using MBE growth.

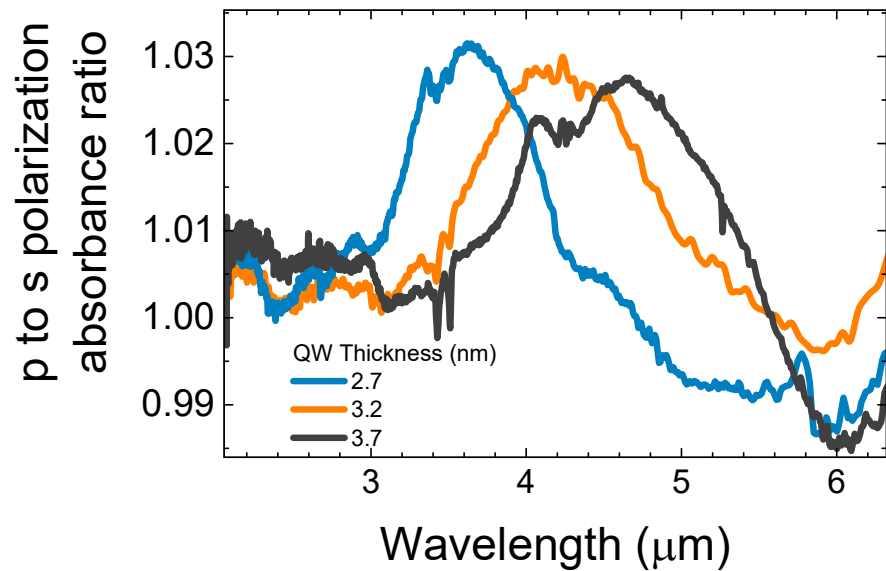


Figure 2. p to s polarization absorbance spectra ratio for the three MQWs presented in this study.

The modeled values for the intersubband transition energies clearly present the same trend with QW thickness, although a sizeable mismatch appears respect to the experimentally obtained values. This difference can only be explained if one accounts for many body effects in the QWs. If we first include the effect of the charge distribution along the QW, we need to solve self consistently Schrödinger and Poisson's equations. When this effect is accounted for, the transitions are shifted to lower values as a result of band bending, as shown in Fig. 3b, compared to the ideal QW potential profile (Fig. 3a). Second, if we also add the effect of exchange correlation between electrons in the QW, the QW band structures is further deformed, now increasing the intersubband transition energies (Fig. 3c).

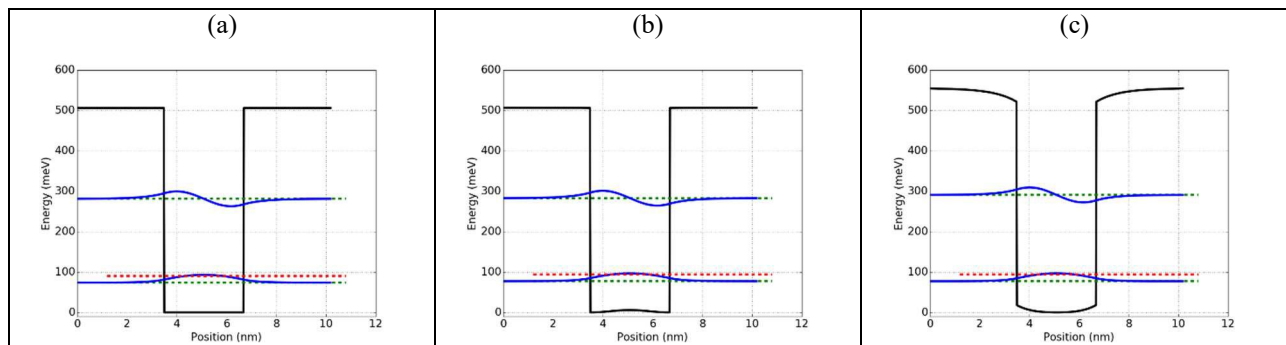


Figure 3. Schematic of one quantum well of the sample presented in this work as calculated from self-consistent solving of: (a) Schrödinger's equation; (b) Schrödinger's and Poisson's; (c) Schrödinger's and Poisson's equations with exchange correlation. The red line indicates de Fermi energy.

However, of all effects, the most important one is the depolarization shift^{10,11}. This effect arises from the screening of the electric field due to the oscillation of the electrons in the QW, and although it typically was quite small in GaAs

intersubband devices, it becomes large here for two reasons. First, the doping level is quite high. Second, the depolarization is driven by the background, high-frequency dielectric constant, which in ZnO is $\epsilon_{\infty} = 3.7$, much lower than that of GaAs (10.9). Thus, the final effect on the intersubband transitions becomes quite large and needs to be accounted for.

Figure 4 shows the experimentally measured intersubband transition energies as a function of the QW thickness and the modeled results. It is clear that while the plain Schrödinger model does not yield a good match with the data, when the effect of the various many body effect mechanisms is accounted for, an excellent matching with the experimental values is obtained.

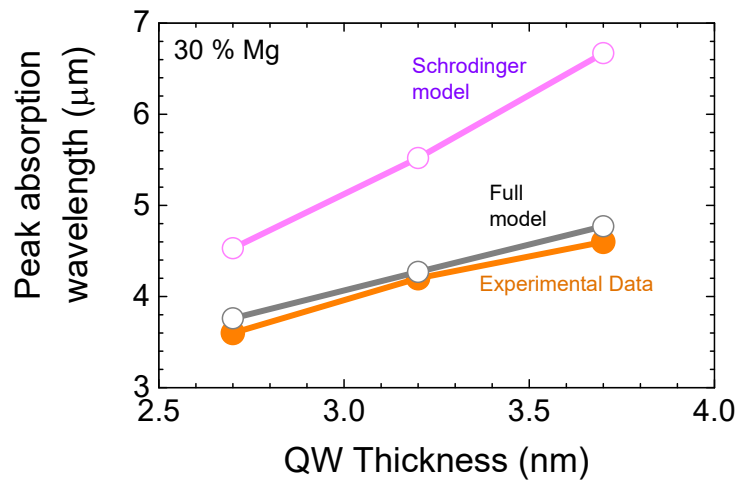


Figure 4. Comparison to the experimental data of the modeled intersubband transition wavelength in the ZnO/ZnMgO MQWs using the basic Schrödinger model, or the full model including many body effects: Poisson, exchange correlation and depolarization shift.

5. CONCLUSIONS

In conclusion, we have shown that intersubband transitions in the mid-IR can be obtained with ZnO/ZnMgO MQWs doped with $1 \times 10^{19} \text{ cm}^{-3}$. By using barriers with 30 % Mg, a careful control of the QW thickness by molecular beam epitaxy from 2.7 to 3.7 nm allows to tune the absorption peak from 3 to 5 μm . These MQWs are homoepitaxially grown on ZnO, allowing to reach films with low defect densities and high optical efficiencies, and use the non-polar m-plane orientation thus avoiding the detrimental effect of the quantum confined Stark effect on the oscillator strength. In order to properly model the band structure of these films, many body effects need to be used since the doping concentrations are high, including Poisson, exchange correlation effects, and depolarization.

ACKNOWLEDGEMENTS

This work was supported by the European Union's Horizon 2020 Research and Innovation Program under grant agreement No. 665107 (project ZOTERAC). Part of the calculations performed here used the Aestimo package.

REFERENCES

- [1] N. Le Biavan, M. Hugues, M. Montes Bajo, J. Tamayo-Arriola, A. Jollivet, D. Lefebvre, Y. Cordier, B. Vinter, F.-H. Julien, A. Hierro, and J.-M. Chauveau, "Homoeptaxy of non-polar ZnO/(Zn,Mg)O multi-quantum wells: From a precise growth control to the observation of intersubband transitions," *App. Phys. Lett.* 111, 231903 (2017).
- [2] M. Montes Bajo, J. Tamayo-Arriola, M. Hugues, J. M. Ulloa, N. Le Biavan, R. Peretti, F. H. Julien, J. Faist, J. M. Chauveau, A. Hierro, "Intersubband polarons in oxides", <https://arxiv.org/abs/1703.07743>, (2017).
- [3] Zhao, K., Chen, G., Li, B. S. and Shen, A., "Mid-infrared intersubband absorptions in ZnO/ZnMgO multiple quantum wells," *App. Phys. Lett.*, 104, 212104 (2014).
- [4] Belmoubarik, M., Ohtani, K. and Ohno, H., "Intersubband transitions in ZnO multiple quantum wells," *App. Phys. Lett.*, 92, 191906 (2008).
- [5] Schneider, H. and Liu, H. C., [Quantum Well Infrared Photodetectors], Springer Berlin Heidelberg, Berlin (2007).
- [6] Özgür, Ü., Alivov, Y. I., Liu, C., Teke, A., Reshchikov, M. A., Doğan, S., Avrutin, V., Cho, S.-. J. and Morkoç, H., "A comprehensive review of ZnO materials and devices," *J. Appl. Phys.*, 98, 041301 (2005).
- [7] J.-M. Chauveau, M. Teisseire, H. Kim-Chauveau, C. Deparis, C. Morhain, and B. Vinter, "Benefits of homoeptaxy on the properties of nonpolar ZnMgO/ZnO quantum wells on a-plane ZnO substrates," *App. Phys. Lett* 97, 081903 (2010).
- [8] M. D. Neumann, N. Esser, J.-M. Chauveau, R. Goldhahn and M. Feneberg, "Inversion of absorption anisotropy and bowing of crystal field splitting in wurtzite MgZnO," *App. Phys. Lett.*, 108, 221105 (2016).
- [9] Yin, H.; Chen, J.; Wang, Y.; Wang, J.; Guo, H., "Composition dependent band offsets of ZnO and its ternary alloys." *Sci. Rep.* 7, 41567 (2017).
- [10] Allen, Jr, S. J.; Tsui, D. C.; Vinter, B., "On the absorption of infrared radiation by electrons in semiconductor inversion layers," *Solid State Commun.* 20, 425 (1976).
- [11] Ando, T.; Fowler, A. B.; Stern, F., "Electronic properties of two-dimensional systems," *Rev. Mod. Phys.* 54, 437 (1982).